

RAPID REMOVAL OF CHROMIUM(VI) FROM AQUEOUS SOLUTION USING IRON OXIDE/POLYANILINE NANOCOMPOSITES

Vu Dinh Thao*, Pham Manh Thao

Department of Physics and Chemical Engineering, Le Quy Don University,

Received 28 March 2015; Accepted for Publication 20 April 2015

Abstract

Core-shell structured magnetic iron oxide nanoparticles/polyaniline (Fe_3O_4 NPs/PANi) nanocomposite has been successfully synthesized by a two-step chemical precipitation-polymerization route, and was characterized using transmission electron microscopy (TEM), Fourier transform infrared spectra (FT-IR), and X-ray diffraction (XRD). Fe_3O_4 NPs/PANi nanocomposite was used as adsorbent to remove hexavalent chromium (Cr(VI)) ions from aqueous solution. The equilibrium data were well fitted the Langmuir isotherm model. The maximum adsorption capacity of Fe_3O_4 NPs/PANi nanocomposite for Cr(VI) is $76.9 \text{ mg}\cdot\text{g}^{-1}$. The adsorption mechanism has been identified as an ion exchange and a redox mechanism, based on X-ray photoelectron spectroscopy (XPS) study. Our study shows that magnetic Fe_3O_4 NPs/PANi nanocomposite is a promising adsorbent for rapid removal of Cr(VI) from aqueous solution.

Keywords. Adsorption, chromium, polyaniline, nanocomposites.

1. INTRODUCTION

Contamination of aquatic media by heavy metals has become a serious environmental problem with the rapid increase in global industrial activities [1]. Among all heavy metals, chromium (Cr) is extensively used in the leather tanning, electroplating, metal finishing and stainless steel industries, and is considered as a high priority environmental pollutant [2]. Cr exists in environment both as trivalent (Cr(III)) and hexavalent (Cr(VI)) forms of which Cr(VI) is roughly 500 times more toxic than Cr(III) [3, 4]. Cr(VI) contamination has caused severe serious health problems such as nausea, diarrhea, liver, kidney damage and lung cancer [5]. Since Cr(VI) is highly toxic, carcinogenic and mutagenic, the World Health Organization has adopted an chromium maximum contaminant level of $0.05 \text{ mg}\cdot\text{L}^{-1}$ in drinking water [6]. The conventional techniques for treatment of Cr(VI) include chemical precipitation, ion exchange, electro-deposition, membrane filtration and adsorption [7]. Among these techniques, adsorption is considered to be effective and economical [8]. Up to now, a variety of adsorbents has been used for Cr(VI) adsorption including activated carbon [9], nanoparticles [10], polymer [11], and biosorbents [12]. In spite of this, the search for new adsorbent materials with high adsorption capacity, low-cost, and easy separation is

still in great demand.

In recent years, magnetic iron oxide nanoparticles (Fe_3O_4 NPs) have been exploited to remove heavy metal ions from water due to their high surface area and unique advantage of easy separation under external magnetic fields [13]. However, bare Fe_3O_4 NPs are strongly susceptible to air oxidation, not stable under acidic conditions and easily aggregated in aqueous solutions [14]. Those disadvantages dramatically reduce adsorption capacity of Fe_3O_4 NPs, especially after recycling. To solve this issue, one of the effective methods is combining Fe_3O_4 NPs with other materials to form magnetic nanocomposites [15].

Polyaniline (PANi) is one of the most important conducting polymers for advanced applications such as photoelectrochemical cells, biosensors, and field-effect transistors [16]. Recently, PANi has been intensively investigated as potential adsorbent for removal of heavy metal ions due to its excellent environmental stability, good redox reversibility, low cost, easy synthesis and treatment, and plenty of amine and imine functional groups [17, 18].

Here, we studied the formation of magnetic Fe_3O_4 NPs/PANi core-shell nanocomposite, its structural properties and the feasible use as an adsorbent towards removal of Cr(VI) from aqueous solution. The cores (Fe_3O_4 NPs) were prepared by a chemical precipitation method and further modified

with p-aminobenzoic acid (AB) for better dispersion into PANi matrix. The shell (PANi) was prepared via a polymerization route in the presence of the cores. We also investigated the adsorption of Cr(VI) on Fe₃O₄ NPs/PANi nanocomposite as a simple method for the removal of Cr(VI) from aqueous solutions.

2. EXPERIMENTAL

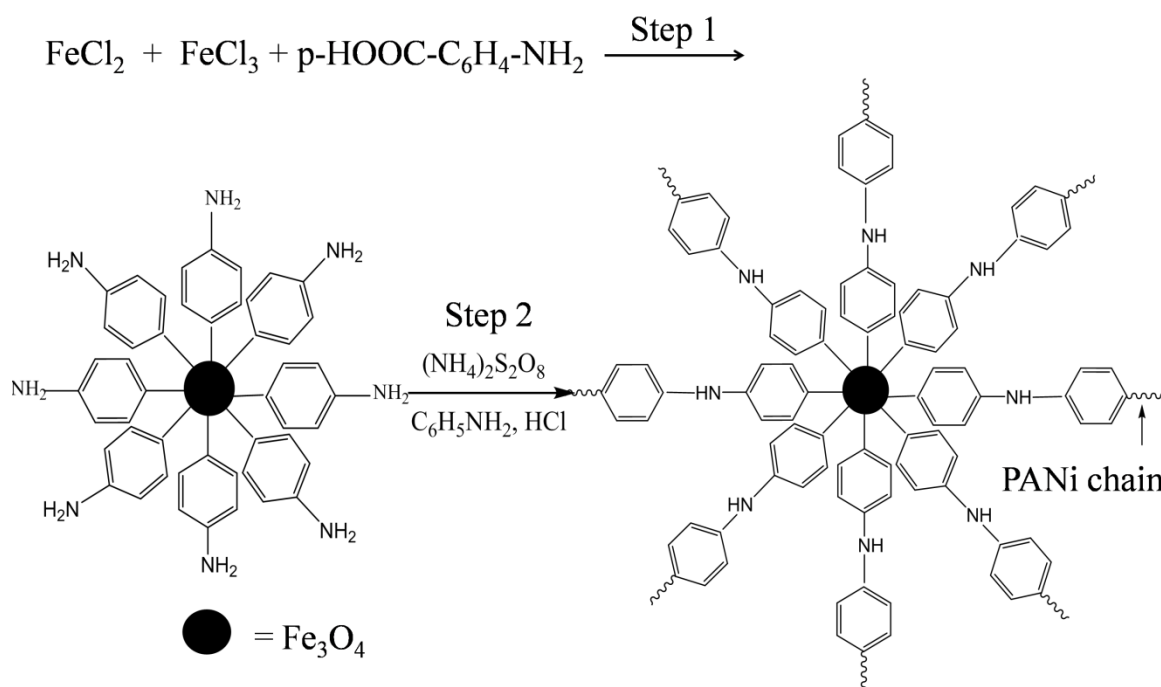
2.1. Materials

Cr (VI) stock solutions (1000 mg.L⁻¹) were prepared from potassium dichromate (K₂Cr₂O₇, Sigma–Aldrich), and were diluted to desired concentrations for various experiments. Aniline monomer, ammonium persulfate (APS), AB were purchased from the Sinopharm Chemical Reagent Co., Ltd. Ferric chloride hexahydrate (FeCl₃.6H₂O, 99 %), ferrous chloride tetrahydrate (FeCl₂.4H₂O, 99 %) and ammonium hydroxide (NH₄OH) were analytical grade reagents and purchased from the Beijing Chemical Company.

2.2. Preparation of core-shell structured Fe₃O₄ NPs/PANi nanocomposite

Core-shell structured Fe₃O₄ NPs/PANi nanocomposite was prepared via the AB-assisted method by a two-step process. In the first step,

Fe₃O₄ NPs were synthesized by a conventional chemical precipitation method [19] followed by functionalization with AB. Briefly, 30 mL of distilled water was deoxygenated by bubbling with N₂ gas for 30 min, then 1.29 g of FeCl₂.4H₂O and 3.52 g of FeCl₃.6H₂O were added. The temperature of the mixture was raised to 60 °C with vigorous stirring for 10 min under N₂ atmosphere. 8.5 mL of NH₄OH (25 %) was rapidly added into the mixture to initiate the precipitation, followed by addition of a solution containing 0.90 g of AB in 5 mL of ethanol, and then the resulting suspension was heated to 80 °C and reacted for another 2 h. The whole process must be under N₂ atmosphere. The reaction mixture was then cooled slowly to room temperature. Fe₃O₄ precipitates were isolated by using an external magnetic field, washed sequentially with distilled water and ethanol for several times to remove the excess of AB, and dried under low pressure at 40 °C for 24 h. In the second step, Fe₃O₄ NPs/PANi nanocomposite was prepared via a polymerization route. 0.45 g of as-prepared Fe₃O₄ NPs/AB was dispersed into 80 mL 0.1M HCl solution under ultrasonication for 30 min, then 0.46 g of aniline was added to the above mixture. A solution of 0.87 g APS in 10 mL 0.1M HCl solution was added quickly and then reacted for 12 h under vigorous stirring conditions. The procedure for isolating Fe₃O₄ NPs/PANi nanocomposite was similar to that of Fe₃O₄ NPs/AB.



Scheme 1: A scheme of the synthesis of Fe₃O₄ NPs/PANi nanocomposite

2.3. Sample characterization

The samples were characterized by transmission electron microscopy (TEM, JEM-2000EX, JEOL, Japan), X-ray diffraction (XRD, Scintag XDS 2000 diffractometer with a $\text{CuK}\alpha$ radiation), Fourier transform infrared spectroscopy (FT-IR, BRUKER VECTOR22), and X-ray photoelectron spectroscopy (XPS, EscalabMkII). The magnetic properties of Fe_3O_4 NPs/PANi nanocomposite were investigated using a vibrating sample magnetometer (VSM, JDM-13) at room temperature.

2.4. Batch adsorption studies

We used Fe_3O_4 NPs and Fe_3O_4 NPs/PANi nanocomposite as adsorbents in batch adsorption studies. All batch experiments were conducted using 0.1 g of adsorbent in a 250 mL conical flask with 100 mL of Cr(VI) aqueous solutions on a rotary shaker at 200 rpm at 25 ± 1 °C. The effect of pH on adsorption was studied in adsorption experiments using 100 mL of Cr(VI) solution ($30 \text{ mg}\cdot\text{L}^{-1}$). Different pH values ranging from 2 to 12 were adjusted by adding 0.1 M NaOH or 0.1 M HCl solutions. In adsorption equilibrium isotherm studies, 0.1 g of adsorbent was mixed with 100 mL of Cr(VI) solution at different concentration ($5\text{-}150 \text{ mg}\cdot\text{L}^{-1}$) and shaken for 240 min at pH 2. After reaching the adsorption equilibrium, the suspension was isolated by using an external magnetic field and

Rapid removal of chromium (VI) from...

the Cr(VI) concentration was analyzed by inductively coupled plasma optical emission spectroscopy (ICP-OES) (Perkin Elmer Optima 7300DV, USA). The adsorption capacity of Cr(VI) was calculated according to the following equation:

$$q_e = \frac{(C_o - C_e)V}{m} \quad (1)$$

where C_o and C_e represent the initial and equilibrium Cr concentration ($\text{mg}\cdot\text{L}^{-1}$), respectively; V is the volume of aqueous solution containing Cr ions (L), and m is the amount of adsorbent (g).

3. RESULTS AND DISCUSSION

3.1. Characterization of Fe_3O_4 NPs/PANi nanocomposite

Figures 1a and b show TEM images of Fe_3O_4 NPs and Fe_3O_4 NPs/PANi, respectively. As seen from Fig. 1a, Fe_3O_4 NPs were almost spherical with an average diameter of about 10 nm. Most of these particles formed aggregates because of the interactions between Fe_3O_4 NPs molecules [20]. In contrary, Fig. 1b shows that Fe_3O_4 NPs were encapsulated in the PANi matrix, forming core-shell structures which were connected with each other to form a network-like system. Fe_3O_4 NPs modified by AB were effectively dispersed into the PANi matrix, and there was little apparent aggregation of Fe_3O_4 NPs in the nanocomposite.

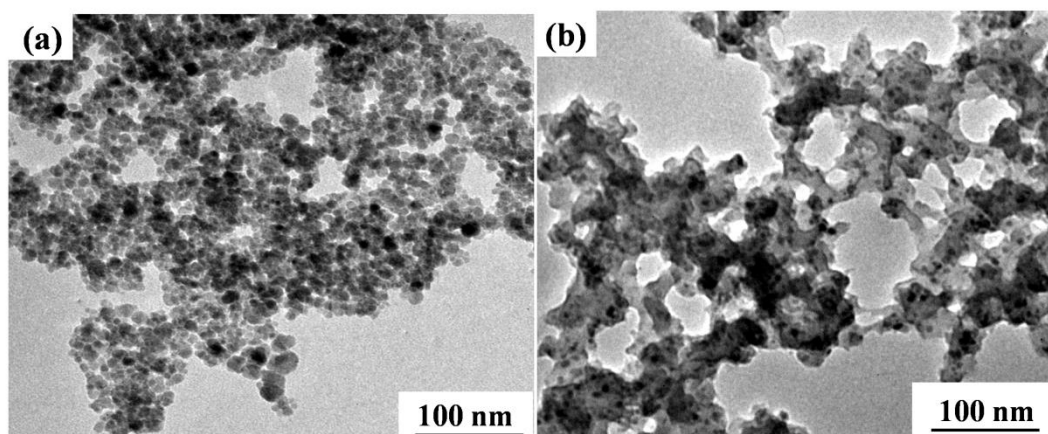


Figure 1: TEM images of (a) Fe_3O_4 NPs and (b) Fe_3O_4 NPs/PANi nanocomposite

The FT-IR spectra of Fe_3O_4 NPs and Fe_3O_4 NPs/PANi are shown in the Fig. 2. In the spectrum of Fe_3O_4 NPs (a), the peak at 1630 cm^{-1} can be assigned to the $\delta(\text{O-H})$ of water molecules adsorbed on the Fe_3O_4 surface. The strong band at 582 cm^{-1} is attributed to characteristic absorption band of Fe-O bonds [21]. In the spectrum of Fe_3O_4 NPs/PANi

nanocomposite (b), strong peaks at 1578 and 1481 cm^{-1} are assigned to the $\nu(\text{C=C})$ in quinoid phenyl ring and $\nu(\text{C=C})$ in benzenoid phenyl ring, respectively. The peak at 1300 cm^{-1} is attributed to $\nu(\text{C-N})$ of a secondary aromatic amine. The peak at 1131 cm^{-1} is from $\nu(\text{C=N})$ of N=Q=N (Q is quinoid ring), the peak at 806 cm^{-1} is assigned to the $\delta(\text{C-H})$

of 1,4-substituted phenyl ring stretch, and the peak at 1242 cm^{-1} is attributed to the $\delta(\text{C-H})$ in benzene plane. All peaks are similar to the IR character of polyaniline synthesized by a conventional method [22]. This result indicates the presence of PANi in nanocomposite.

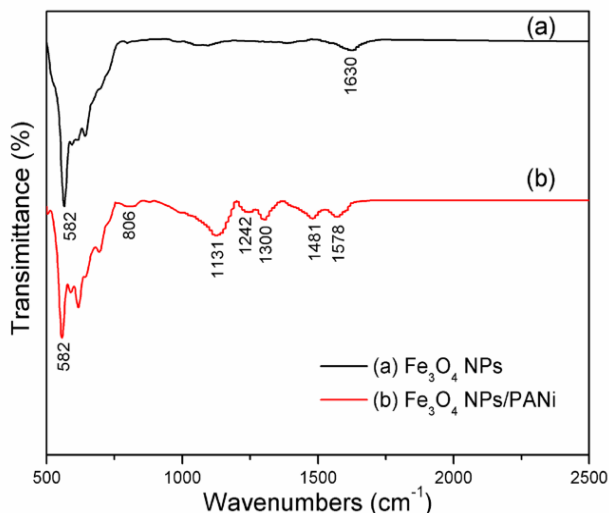


Figure 2: FT-IR spectra of (a) Fe_3O_4 NPs and (b) Fe_3O_4 NPs/PANi nanocomposite

The characteristic peaks of Fe_3O_4 NPs modified with AB cannot be clearly seen from FT-IR spectra. Therefore, we used XPS to examine the existence of AB on the Fe_3O_4 NPs surface. Fig. 3 shows a survey XPS spectrum of Fe_3O_4 NPs/AB. The appearance of N 1s peak at binding energy 399.6 eV is assigned to the amine group ($-\text{NH}-$). In addition, the presence of C 1s peak at 284.8 eV, O 1s peak at 530.4 eV and Fe 2p peaks at 710.5 and 723.7 eV all confirmed that AB was absorbed on the Fe_3O_4 NPs surface.

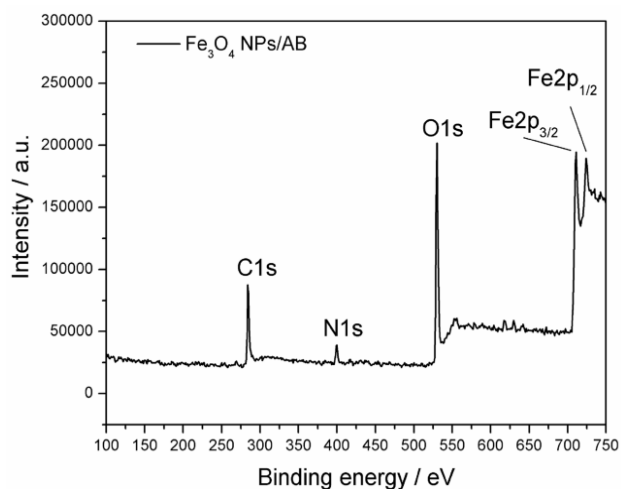


Figure 3: XPS spectra of Fe_3O_4 NPs/AB nanocomposite

The XRD patterns of Fe_3O_4 NPs, Fe_3O_4 NPs/AB

and Fe_3O_4 NPs/PANi are shown in Fig. 4. All samples exhibited six characteristic peaks at $2\theta=30.10$ (220), 35.40 (311), 43.10 (400), 53.50 (422), 57.10 (511), and 62.70 (440). All diffraction peaks can be accurately indexed as the spinel structure for standard Fe_3O_4 crystal (JCPDS card #19-0629). It indicates that the modification of Fe_3O_4 NPs with AB and PANi did not alter its crystalline structure.

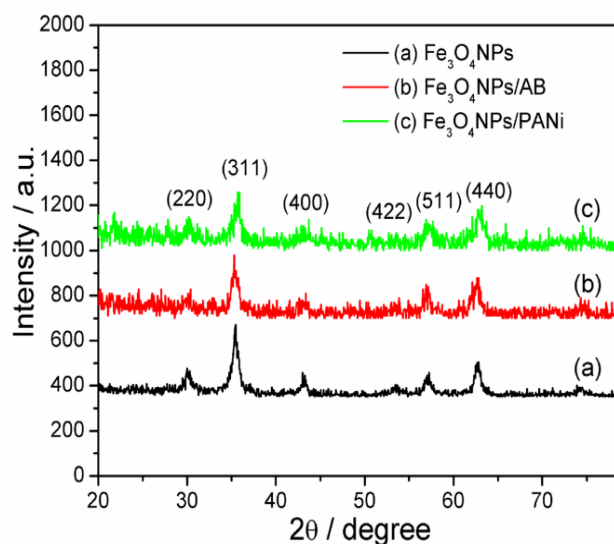


Figure 4: XRD patterns of (a) Fe_3O_4 NPs, (b) Fe_3O_4 NPs/AB and Fe_3O_4 NPs/PANi nanocomposite

The magnetization curves measured for Fe_3O_4 NPs and Fe_3O_4 NPs/PANi are presented in Fig. 5a. The saturated magnetization (M_s) values were measured to be $80\text{ emu}\cdot\text{g}^{-1}$ for Fe_3O_4 NPs and $20\text{ emu}\cdot\text{g}^{-1}$ for Fe_3O_4 NPs/PANi nanocomposite. No hysteresis loop was observed, indicating that both Fe_3O_4 NPs and Fe_3O_4 NPs/PANi nanocomposite were superparamagnetic [23, 24]. This superparamagnetic behavior suggests that a simple and rapid separation of magnetic Fe_3O_4 NPs/PANi nanocomposite from treated water can be achieved under an external magnetic field. As shown in Fig. 5c, the initial black Cr(VI) solution containing homogeneously dispersed Fe_3O_4 NPs/PANi nanocomposite became clear after 2 min when placed near a permanent magnet and complete magnetic separation of Fe_3O_4 NPs/PANi nanocomposite from the solution was achieved within 5 min (Fig. 5d). Simultaneously, the solution became transparent, indicating high adsorption efficiency of Fe_3O_4 NPs/PANi nanocomposite toward Cr(VI). Compared to conventional solid-liquid separation methods [25], this nanocomposite material displayed many advantages such as simplicity, high speed, and easy control.

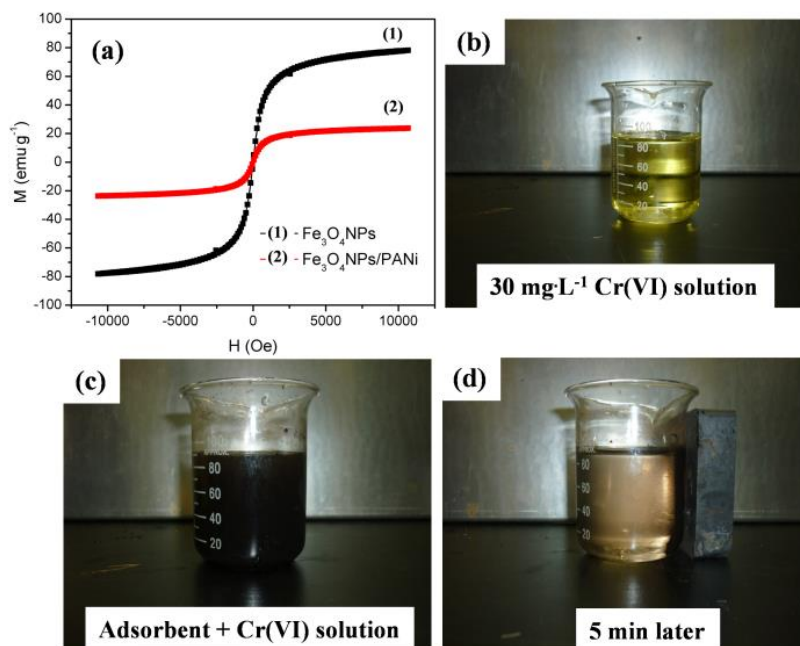


Figure 5: Magnetization curves of Fe₃O₄ NPs and Fe₃O₄ NPs/PANi nanocomposites (a). Photos of as-prepared Cr(VI) solution at a concentration of 30 mg·L⁻¹ (b), immediately after adding Fe₃O₄ NPs/PANi nanocomposite (c) and after 5 min (d)

3.2. Adsorption behavior

3.2.1. Effect of pH

The pH of the aqueous solution is an important controlling parameter in the adsorption process. In this study, the effect of pH (2.0 ≤ pH ≤ 12) on the adsorption was evaluated in the following conditions: 0.1 g of adsorbent in 100 ml of Cr(VI) solution (30 mg·L⁻¹), equilibrium time of 240 min. As presented in Fig. 6, at any pH values, the adsorption efficiency of Cr(VI) onto Fe₃O₄ NPs/PANi nanocomposite is always higher than that of Fe₃O₄ NPs. Obviously, the incorporation of Fe₃O₄ NPs into PANi matrix dramatically enhances its adsorption capacity. Adsorption efficiency of Cr(VI) onto Fe₃O₄ NPs/PANi nanocomposite decreases with increasing pH from 2.0 to 12 (maximum efficiency at pH of 2.0). To explain this phenomenon, it is necessary to recall that Cr(VI) exists mainly in the form of HCrO₄⁻ and Cr₂O₇²⁻ at acidic pH (2.0-6.0), and as CrO₄²⁻ at pH > 6.0. The higher adsorption efficiency in the acidic pH (2.0-6.0) is due to the anion exchange property of the Fe₃O₄ NPs/PANi nanocomposite by replacing the doped Cl⁻ and SO₄²⁻ ions with either HCrO₄⁻ and Cr₂O₇²⁻ ions. In the alkaline pH (8.0-12), the significant decrease of the Cr(VI) uptake with the increase of pH values is due to the increased concentration of OH⁻ ions presenting in the reaction

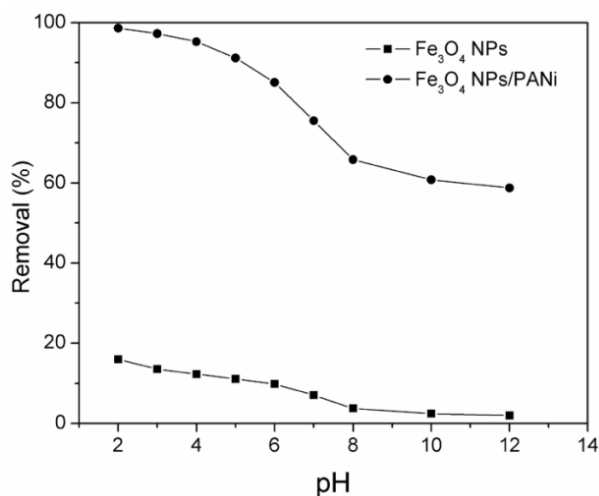


Figure 6: Effect of pH on the adsorption of Cr(VI) onto Fe₃O₄ NPs and Fe₃O₄ NPs/PANi. In the pH range of 2.0-12, dosage of adsorbent: 1 g·L⁻¹, adsorption equilibrium time: 240 min. Initial Cr (VI) concentration of 30 mg·L⁻¹

mixture, which compete with Cr(VI) anions for the adsorption sites on Fe₃O₄ NPs/PANi nanocomposite. In the same condition, Cr(VI) ions removal by Fe₃O₄ NPs decreases from 16.7 % (pH 2.0) to 10.27 % (pH 6.0) and 2.2 % (pH 12). This result can be explained by considering the surface charge on adsorbent material. The point of zero charge (pH_{pzc}) of Fe₃O₄ NPs determined in previous studies [26] was

6.8. When pH is lower than pH_{pzc} , Fe_3O_4 surface is positively charged ($FeOH + H^+ \rightarrow FeOH_2^+$) and becomes favorable for the adsorption of negatively charged $HCrO_4^-$ and $Cr_2O_7^{2-}$ anions. On the other hand, when pH is higher than pH_{pzc} , Fe_3O_4 surface is negatively charged ($FeOH + OH^- \rightarrow FeO^- + H_2O$) and becomes unfavorable for the adsorption of negatively charged CrO_4^{2-} anions due to electrostatic repulsion. After investigation of effect of pH, we chose the pH of 2.0 for subsequent studies.

3.2.2. Adsorption isotherms

The adsorption equilibrium data were analyzed using Langmuir and Freundlich isotherm models. Langmuir isotherm [27] assumes monolayer adsorption onto a surface containing a finite number of adsorption sites with no transmigration of adsorbate in the plane of surface. The linearized Langmuir isotherm equation is given as:

$$\frac{C_e}{q_e} = \frac{C_e}{q_m} + \frac{1}{q_m K_L} \quad (2)$$

where q_e and C_e are the adsorption capacity ($mg.g^{-1}$) and concentration of Cr(VI) ($mg.L^{-1}$) at equilibrium, respectively; q_m and K_L represent the maximum adsorption capacity of adsorbents ($mg.g^{-1}$) and the Langmuir constant ($L.mg^{-1}$), respectively. The values of q_m and K_L were calculated from the slope and intercept of the linear plot of C_e/q_e versus C_e , as shown in Fig. 7.

The Freundlich isotherm [28] is an empirical equation which is used to describe adsorption at multilayer and adsorption on a heterogeneous surface. It is expressed by the following linear form:

$$\log q_e = \log K_f + \frac{1}{n} \log C_e \quad (3)$$

Where K_f and n are Freundlich isotherm constants which are related to the adsorption capacity and the adsorption strength of the adsorbent, respectively. K_f and n can be obtained from the intercept and the slope of the linear plot of $\log(q_e)$ versus $\log(C_e)$, as shown in Fig. 8.

Table 1: Calculated parameters of the Langmuir and Freundlich isotherm models

Adsorbent	Freundlich isotherm			Langmuir isotherm		
	n	K_f	R^2	q_m (mg/g)	K_L (L/mg)	R^2
Fe_3O_4 NPs	5.09	2.48	0.9824	5.04	0.43	0.9951
Fe_3O_4 NPs/PANi	6.37	39.65	0.9583	76.92	0.52	0.9972

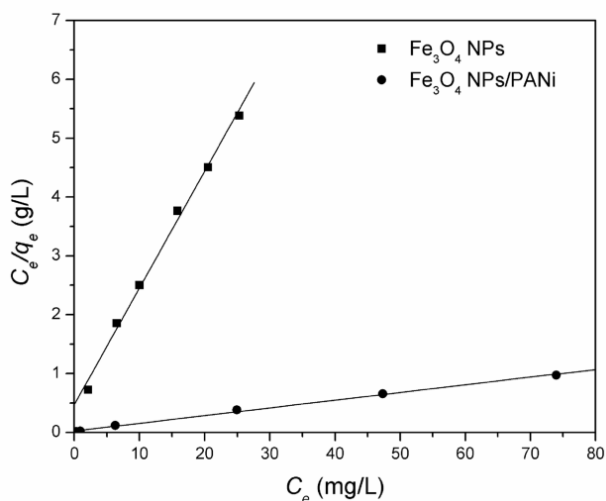


Figure 7: Adsorption isotherm of Cr (VI) onto Fe_3O_4 NPs and Fe_3O_4 NPs/PANi (Linearized Langmuir equations) at $T = 25$ °C, pH 2.0, dosage of adsorbent: $1 g.L^{-1}$

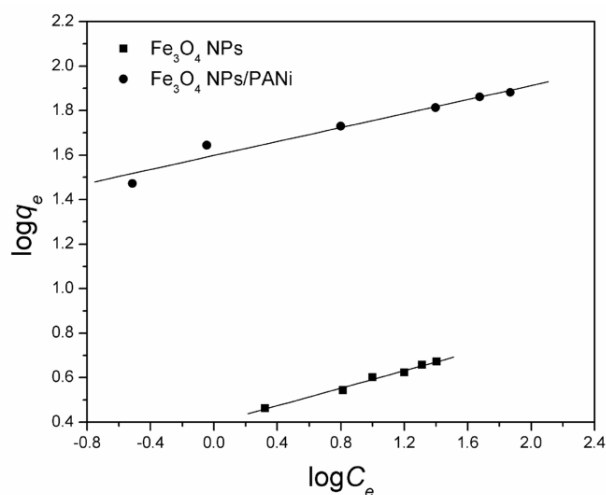


Figure 8: Adsorption isotherm of Cr (VI) onto Fe_3O_4 NPs and Fe_3O_4 NPs/PANi (Linearized Freundlich equations) at $T = 25$ °C, pH 2.0, dosage of adsorbent: $1 g.L^{-1}$

The results obtained from adsorption isotherms for Cr(VI) adsorption onto Fe₃O₄ NPs/PANi were summarized in table 1. As shown in the table, the Langmuir correlation coefficients (R^2) of Cr(VI) adsorption onto adsorbents were higher than those of Freundlich's model, suggested that the adsorption of Cr(VI) onto both adsorbents is a monolayer adsorption. The maximum adsorption capacity (q_m) calculated from the linearized Langmuir equation of Fe₃O₄ NPs/PANi (76.9 mg.g⁻¹) was much higher than that of Fe₃O₄ NPs (5.04 mg.g⁻¹). Obviously, the enhancement of adsorption of Cr (VI) by Fe₃O₄ NPs/PANi was because of excellent adsorption property of PANi and Fe₃O₄ NPs/PANi nanocomposite could be used as an effective adsorbent material for treatment of Cr(VI) in aqueous solution.

3.2.3. Mechanism of Cr(VI) adsorption

In mechanism study, the adsorption of Cr (VI) onto Fe₃O₄ NPs/PANi nanocomposite was conducted at following conditions: pH 2; t = 25 °C; dosage of adsorbent: 1 g.L⁻¹; and initial Cr (VI) concentration: 30 mg.L⁻¹. Fig. 9 shows XPS spectra for magnetic Fe₃O₄ NPs/PANi nanocomposite before and after Cr(VI) adsorption. The binding energy values at 168.3, 198.6 and 400.5 eV correspond to S 2p, Cl 2p and N 1s of functional group (-N⁺), indicating the doping of Cl⁻ and SO₄²⁻ anions into Fe₃O₄ NPs/PANi nanocomposite. The XPS spectrum of Fe₃O₄ NPs/PANi nanocomposite after Cr(VI) adsorption (b) shown that the Cl peak and the S peak disappeared. However, the new two Cr peaks at 577.1 eV and 587.9 eV were observed. This feature indicates that the adsorption Cr(VI) ions onto Fe₃O₄ NPs/PANi nanocomposite may be by replacing doping Cl⁻ and SO₄²⁻ anions. Moreover, the two peaks centered at 577.1 eV and 587.9 eV are assigned to Cr 2p_{3/2} (Cr(III)) and Cr 2p_{1/2} (Cr(VI)), respectively (the inset, c). The simultaneous existence of Cr(VI) and Cr(III) on the adsorbent surface indicates that Cr(VI) is reduced to Cr(III) during or after the adsorption ($\text{HCrO}_4^- + 7\text{H}^+ + 3\text{e}^- \rightarrow \text{Cr}^{3+} + 4\text{H}_2\text{O}$). As supported by the FT-IR study, the PANi contains electron-rich aromatic ring structures and nitrogen-containing functional groups. These structures and functional groups act as electron donors for reduction of Cr(VI) to Cr(III).

4. CONCLUSIONS

Core-shell structured magnetic Fe₃O₄ NPs/PANi nanocomposite has been successfully synthesized

and used as an efficient and low-cost adsorbent for the removal of Cr(VI) from aqueous solutions. The adsorption capacity of Fe₃O₄ NPs/PANi nanocomposite was remarkably higher than that of Fe₃O₄ NPs. The adsorption of Cr(VI) onto Fe₃O₄ NPs/PANi follows Langmuir isotherm model. Ion exchange and reduction on the Fe₃O₄ NPs/PANi nanocomposite is a possible mechanism for Cr(VI) removal. The separation of Fe₃O₄ NPs/PANi nanocomposite from the treated water was rapid and simple using an external magnetic field. The present work demonstrated a simple method for fabrication of efficient and low-cost magnetic adsorbent for removal of Cr(VI) from aqueous solutions.

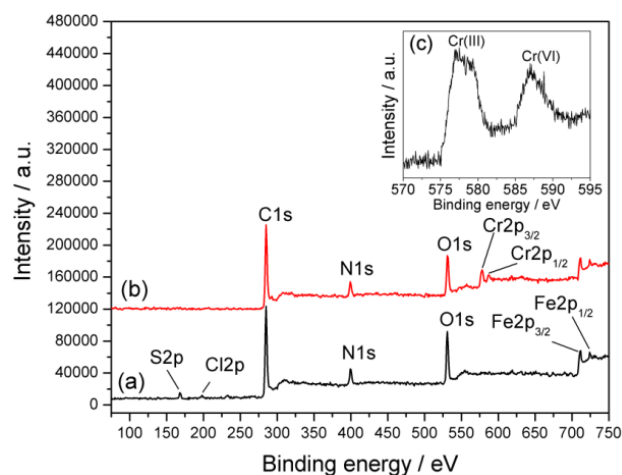


Figure 9: XPS survey spectra of Fe₃O₄ NPs/PANi before (a) and after adsorption (b). Inset (c): XPS analysis of Fe₃O₄ NPs/PANi nanocomposite after Cr(VI) adsorption

REFERENCES

1. V. D. Thao, Z. Li, H. Zhang, W. Wang, Z. Wang, X. Xu, B. Dong, and C. Wang. *Adsorption of Cu(II) from aqueous solution by anatase mesoporous TiO₂ nanofibers prepared via electrospinning*, J. Colloid Interface Sci, **367**, 429-435 (2012).
2. R. Ansari and N. K. Fahim. *Application of polypyrrole coated on wood sawdust for removal of Cr(VI) ion from aqueous solutions*, React. Funct. Polym., **67**, 367-374 (2007).
3. V. K. Gupta and S. Agarwal, T. A. Saleh. *Chromium removal by combining the magnetic properties of iron oxide with adsorption properties of carbon nanotubes*, Water Res., **45**, 2207-2212 (2011).
4. V. Sarin and K. K. Pant. *Removal of chromium from industrial waste by using Eucalyptus Bark*, Bioresour. Technol., **97**, 15-20 (2006).
5. K. Pillay, E. M. Cukrowski, and N. J. Coville. *Multi-walled carbon nanotubes as adsorbents for the removal of parts per billion levels of hexavalent chromium from aqueous solution*, J. Hazard Mater.,

- 166**, 1067-1075 (2009).
6. Y. G. Abou El-Reash, M. Otto, I. M. Kenawy, and A. M. Ouf. *Adsorption of Cr(VI) and As(III) ions by modified magnetic chitosan chelating resin*, Int. J. Biol. Macromol., **49**, 513-522 (2011).
 7. M. K. Aroua, F. M. Zuki, and N. M. Sulaiman. *Removal of chromium ions from aqueous solutions by polymer-enhanced ultrafiltration*, J. Hazard. Mater., **147**, 752-758 (2007).
 8. D. Mohan and C. U. Pittman Jr. *Activated carbons and low cost adsorbents for remediation of tri- and hexavalent chromium from water*, J. Hazard Mater., **137**, 762-811 (2006).
 9. S. X. Liu, X. Chen, X. Y. Chen, Z. F. Liu, and H. L. Wang. *Activated carbon with excellent chromium (VI) adsorption performance prepared by acid-base surface modification*, J. Hazard. Mater., **141**, 315-319 (2007).
 10. P. Wang and I. M. C. Lo. *Synthesis of mesoporous magnetic γ -Fe₂O₃ and its application to Cr(VI) removal from contaminated water*, Water Res., **43**, 3727-3734 (2009).
 11. Y. G. Ko, Y. J. Chun, C. H. Kim, and U. S. Choi. *Removal of Cu(II) and Cr(VI) ions from aqueous solution using chelating fiber packed column: Equilibrium and kinetic studies*, J. Hazard. Mater., **194**, 92-99 (2011).
 12. L. Wei, G. Yang, R. Wang, and W. Ma. *Selective adsorption and separation of chromium (VI) on the magnetic iron-nickel oxide from waste nickel liquid*, J. Hazard Mater., **164**, 1159-1163 (2009).
 13. J. Hu, G. Chen, and I. M. C. Lo. *Selective removal of heavy metals from industrial wastewater using maghemite nanoparticle: performance and Mechanisms*, J. Environ. Eng., **132**, 709-715 (2006).
 14. D. Maity and D. C. Agrawal. *Synthesis of iron oxide nanoparticles under oxidizing environment and their stabilization in aqueous and non-aqueous media*, J. Magn. Mater., **308**, 46-55 (2007).
 15. Y. G. Zhao, H. Y. Shen, S. D. Pan, and M. Q. Hu. *Synthesis, characterization and properties of ethylenediamine-functionalized Fe₃O₄ magnetic polymers for removal of Cr(VI) in wastewater*, J. Hazard. Mater., **182**, 295-302 (2010).
 16. J. Wang, S. Zheng, Y. Shao, J. Liu, Z. Xu, and D. Zhu. *Amino-functionalized Fe₃O₄@SiO₂ core-shell magnetic nanomaterial as a novel adsorbent for aqueous heavy metals removal*, J. Colloid Interface Sci., **349**, 293-299 (2010).
 17. W. Wang, Z. Li, X. Xu, B. Dong, H. Zhang, Z. Wang, C. Wang, R. H. Baughman, and S. Fang. *Au-doped polyacrylonitrile-polyaniline core-shell electrospun nanofibers having high field-effect mobilities*, Small, **7**, 597-600 (2011).
 18. D. Shao, C. Chen, and X. Wang. *Application of polyaniline and multiwalled carbon nanotube magnetic nanocomposites for removal of Pb(II)*, Chem. Eng. J., **185**, 144-150 (2012).
 19. X. J. Hu, J. S. Wang, Y. G. Liu, X. Li, G. M. Zeng, Z. L. Bao, X. X. Zeng, A. W. Chen, and F. Long. *Adsorption of chromium (VI) by ethylenediamine-modified cross-linked magnetic chitosan resin: Isotherms, kinetics and thermodynamics*, J. Hazard Mater., **185**, 306-314 (2011).
 20. J. F. Liu, Z. S. Zhao, and G. B. Jiang. *Coating Fe₃O₄ magnetic nanoparticles with humic acid for high efficient removal of heavy metals in water*, Environ. Sci. Technol., **42**, 6949-6954 (2008).
 21. M. Xu, Y. Zhang, Z. Zhang, Y. Shen, M. Zhao, and G. Pan. *Study on the adsorption of Ca²⁺, Cd²⁺ and Pb²⁺ by magnetic Fe₃O₄ yeast treated with EDTA dianhydride*, Chem. Eng. J., **168**, 737-745 (2011).
 22. H. Guo, H. Zhu, H. Lin, and J. Zhang. *Polyaniline/Fe₃O₄ nanocomposites synthesized under the direction of cationic surfactant*, Mater. Lett., **62**, 2196-2199 (2008).
 23. C. T. Yavuz, J. T. Mayo, W. W. Yu, A. Prakash, J. C. Falkner, S. Yean, L. Cong, H. J. Shipley, A. Kan, M. Tomson, D. Natelson, and V. L. Colvin. *Low-field magnetic separation of monodisperse Fe₃O₄ nanocrystals*, Science, **314**, 964-967 (2006).
 24. S. Yean, L. Cong, C. T. Yavuz, J. T. Mayo, W. W. Yua, A. T. Kan, V. L. Colvin and M. B. Tomson. *Effect of magnetite particle size on a adsorption and desorption and arsenate*, J. Mater. Res., **20**, 3255-3264 (2011).
 25. Z. G. Peng, K. Hidajat, and M. S. Uddin. *Adsorption of bovine serum albumin on nanosized magnetic particle*, J. Colloid Interface Sci., **271**, 277-283 (2004).
 26. W. Yang, A. T. Kan, W. Chen, and M. B. Tomson. *pH-dependent effect of zinc on arsenic adsorption to magnetite nanoparticles*, Water Res., **44**, 5693-5701 (2010).
 27. I. Langmuir. *The adsorption of gases on plane surfaces of glass, mica and Platinum*, J. Am. Chem. Soc., **40**, 1361-1403 (1918).
 28. F. R. Balcar, G. Stegeman. *Über die Adsorption in Lösungen*, Zeitschrift für Physikalische Chemie (Leipzig). J. Phys. Chem., **32**, 1411-1421 (1928).

Corresponding author: **Vu Dinh Thao**

Department of Physics and Chemical Engineering
 Le Quy Don University, 236 Hoang Quoc Viet, Hanoi, Vietnam
 E-mail: vudinhthao81@gmail.com; Phone: 0982755524.